Intravital microscopy at the single vessel level brings new insights of vascular modification mechanisms induced by electropermeabilization

Elisabeth Bellard [a,b,1], Bostjan Markelc [c,1], Sandrine Pelofy [a,b], François Le Guerroué [a,b], Gregor Sersa [c], Justin Teissié [a,b], Maja Cemazar [c,d,*], Muriel Golzio [a,b,**]

[a] CNRS, IPBS (Institut de Pharmacologie et de Biologie Structurale), BP 64182, 205 Route de Narbonne, F-31077, Toulouse, France
[b] Université de Toulouse, UPS (Université Paul Sabatier), IPBS (Institut de Pharmacologie et de Biologie Structurale), BP 64182, F-31077, Toulouse, France
[c] Department of Experimental Oncology, Institute of Oncology Ljubljana, Zaloska 2, SI-1000 Ljubljana, Slovenia
[d] University of Primorska, Faculty of Health Sciences, Polje 42, SI-6310 Izola, Slovenia

ABSTRACT

Electroporation/electropermeabilization, *i.e.* the result of the application of electric pulses to tissues, is a physical method for delivery of exogenous molecules into cells. It is effective particularly for compounds with limited transmembrane transport. *In vivo*, electropermeabilization facilitates the delivery of chemotherapeutic drugs into tumor cells that is the basic mechanism of the antitumor effectiveness of electrochemotherapy. This therapy has also blood flow modifying effects in tissues. The aim of our present study was to understand and explain the effects of electropermeabilization on the dynamics (vasomotricity, permeability and recovery) of subcutaneous blood vessels towards different size of molecules. These features were measured in C57Bl/6 mice *via* a dorsal skin fold window chamber, using fluorescently labeled dextrans of different sizes, intravital fluorescence microscopy imaging and specific image analysis. Application of electric pulses on the skin *in vivo* resulted in a rapid increase in vascular permeability that gradually recovered to basal levels at different times post-treatment, depending on dextran size. Simultaneously, the immediate constriction of the blood vessels occurred that was more pronounced for arterioles compared to venules. This vasoconstriction of arterioles results in a transient "vascular lock".

The increased permeability of small vessels walls whatever the dextran size associated with delayed perfusion explains the improved delivery of the intravenous injected molecules (*i.e.* drugs, gene delivery) into the tissues induced by electropermeabilization *in vivo*.

© 2012 Elsevier B.V. All rights reserved.

1. Introduction

Electroporation/electropermeabilization (EP), *i.e.* application of electric pulses to cells or tissues, induces reversible permeabilization of cell membranes under suitable conditions, thus facilitating entry into the cells of non-permeant or poorly permeant molecules [1]. Biological responses and associated techniques have a broad spectrum of biomedical applications, such as gene and cytotoxic drug delivery [2–4]. EP of tissues in humans is feasible, efficient and tolerable and its most advanced routine clinical use is electrochemotherapy (ECT). The cytotoxicity of bleomycin and cisplatin is potentiated by increased drug delivery into tumor cells by EP that results in up to 80% of complete responses in different tumor types [5]. Reversible permeabilization of cell membrane due to EP is the basic mechanism of the antitumor effectiveness of ECT [5–10]. Nowadays, EP is also increasingly used for the delivery of different nucleic acids (plasmid DNA, siRNA, miRNA, and shRNA) into cells *in vitro* and also into different tissues *in vivo*, including muscle, skin and tumors. This application is termed electrogenetherapy [11–16] where clinical trials with electrotransfer of IL-12 in melanoma patients showed positive results [17,18].

In addition to the improved delivery of exogenous molecules to tissues, it has been observed that EP has blood modifying effects in tumors and normal tissues [19–21]. Different indirect techniques have been used for measuring blood flow changes after EP used in ECT of tumors and electrogene therapy applied to muscles [22–25]. In tumors, a significant reduction of blood volume has been evaluated after EP [21] without any systemic change in blood flow in normal tissue [24]. Thus, EP appears to be a tumor blood flow modifying approach that acts locally, without systemic vascular effects. Clearance of the drug from tumors impeded by reduced blood flow may improve its delivery into the permeabilized tumor cells. In muscles, the effect on perfusion is short-lived compared to tumors [19].

* Correspondence to: M. Cemazar, Department of Experimental Oncology, Institute of Oncology Ljubljana, Zaloska 2, SI-1000 Ljubljana, Slovenia. Tel.: +386 15879544; fax: +386 15879434.
** Correspondence to: M. Golzio, IPBS CNRS, UMR 5089, 205, Route de Narbonne, 31077 Toulouse Cedex, France. Tel.: +33 561175812; fax: +33 561175994.
E-mail addresses: mcemazar@onko-i.si (M. Cemazar), muriel.golzio@ipbs.fr (M. Golzio).
[1] These authors contributed equally to this work.

Investigation of the reversible effects of EP on the cytoskeleton of cultured primary endothelial cells *in vitro* has shown that EP results in a loss of contractility and in a disruption of the barrier function of the endothelium by interacting with the cytoskeletal organization and integrity of cell junctions [26].

Using the combination of high voltage (HV) and low voltage (LV) pulses protocol for plasmid DNA electrotransfer to the skin, we previously showed that EP induced a transient constriction and increased permeability of blood vessels as well as a "vascular lock". We demonstrated that these blood flow modifying effects of EP in the skin contributed to the infiltration of immune cells in the exposed area [27]. When combined with local injection of plasmid DNA for vaccination, this could enable the initial and prolonged contact of immune cells with encoded therapeutic proteins [28].

However, for the validated protocol used in biomedical applications (8 pulses, 100 μs duration, 1300 V/cm, 1 Hz), the effect of EP on drug delivery to the target tissue *via* blood vessels remains poorly addressed [29,30]. Only one study showed that the expression of genes can be achieved after an intravenous injection of plasmid DNA and subsequent application of electric pulses to different tissues including the skin in mice. Although the expression levels were lower in comparison to the levels achieved with direct injection of plasmid DNA into the tissue and subsequent application of electric pulses, they were still statistically relevant if compared to the intravenous injection only [28]. However, how the delivery of molecules modulated by the EP-induced vascular lock and increased permeability of blood vessels for different sizes of molecules still remains to be explained.

In order to observe directly, at the single blood vessel level, the effects of electric pulses on the dynamics (vasomotricity, permeability and recovery) of subcutaneous blood vessels and the subsequent delivery of molecules with increasing sizes in the surrounding tissue, an *in vivo* analysis was performed on dorsal window chambers (DWC) of mice using intravital fluorescence digitized microscopy imaging [27,31]. For this purpose, electric pulses were delivered directly to the skin. We used fluorescein isothiocyanate (FITC) labeled dextrans (FD) of different sizes to mimic different molecules and study the temporal and spatial changes in normal blood vessel morphology and dynamics after EP.

2. Materials and methods

2.1. Animals

Adult female C57Bl/6 mice (Charles River Laboratories, France or Institute of Pathology, Faculty of Medicine, University of Ljubljana, Slovenia) weighing between 21 and 26 g were used as host for DWC preparations. All animal experiments were conducted in accordance with French procedural guidelines for animal handling and with approval from the Regional Ethical Review Committee (MP/02/36/10/10) or in accordance with the official guidelines and approval of the Ministry of Agriculture, Forestry and Food of the Republic of Slovenia (permission No.: 34401-12/2009/6).

2.2. Reagents

Fluorescein isothiocyanate (FITC) labeled dextrans (FD) (20, 70 and 2000 kDa) were purchased from Sigma Chemical Co. (St. Louis, MO). They were dissolved in phosphate-buffered saline (PBS) and washed through 10, 30 and 1000 kDa spin filters (Sartorius Stedim Biotech GmbH, Goettingen, Germany) at 3000 rpm to remove any free FITC or low molecular weight contaminants. The high molecular weight component was resuspended in PBS at 37.5 mg/ml concentration and used in mice at 3.75 mg/100 μl.

2.3. DWC surgery

Surgery was carried out under general anaesthesia using intra peritoneal injection of Ketamine (1 mg/ml, MERIAL, Lyon, France or Narketan®, Vetoquinol AG, Ittigen, Switzerland), Xylazine (5 mg/ml, Bayer, Puteaux, France or Chanazine, Chanelle Pharmaceuticals Manufacturing Ltd, Loughrea, Ireland) and Acepromazyne (0.4 mg/ml, Promace, Fort Dodge Animal Health, Iowa, USA). Briefly, animals were kept warm using heating pads and an aseptic technique was used throughout the surgical procedure. The DWC consisted of two symmetrical titanium frames (APJ Trading Co., Ventura, CA, USA). These frames sandwiched an extended double layer of dorsal skin with the use of stainless steel screws and sutures. After the implantation of the frames, one layer of the skin (12 mm diameter) was surgically removed to create an observation window. After addition of sterile PBS, a sterile glass coverslip was attached to the open frame with a stainless steel clip to cover the surgical site and provide visual access to the vascular network of the skin [32]. After the surgery and on the following day, Profenid (Sanofi-Aventis, Paris, France) was injected, intramuscularly, to provide analgesia and to avoid inflammation (10 mg/kg, 50 μl in each thigh).

2.4. Study design

EP was carried out three to 14 days following surgery, by application of eight square electric pulses, amplitude per distance 1300 V/cm, pulse length 100 μs, repetition frequency 1 Hz, generated by an electropulsator (Jouan GHT, St Herblain, France; or Cliniporator™, IGEA s.r.l., Carpi, Italy). Pulses were delivered by two parallel stainless steel rods (length 5 mm, width 1.3 mm) 4 mm apart, which were placed in contact with the intact skin on the opposite side of the cover glass. Good contact was assured by means of conductive gel (Eko-gel, Egna, Italy). Mice in which no EP was applied served as a control group. FDs were injected in the retro-orbital plexus. FDs were injected either before EP to observe extravasation of FDs into the tissue, or at different times post-EP to observe the "resealing" of the vessel walls.

2.5. Intravital microscopy and image acquisition

Intravital microscopy was carried out on a customized stage for holding mice using an upright "Macrofluo" fluorescence macroscope (Leica Microsystems SA, Rueil-Malmaison, France), equipped with a Cool Snap HQ Camera (Roper Scientific, Photometrics, Tucson, AZ, USA), or a Zeiss SteREO Lumar.V12 (Zeiss, Jena, Germany) fluorescence stereomicroscope equipped with a MRc.5 digital camera (Zeiss). Animals were anaesthetized with inhalation anaesthesia (Isofluran, Nicholas Piramal India LTD, London, UK or Belamont, Neuilly sur Seine, France) throughout the experiment. Vessels were imaged by fluorescence using appropriate filters (excitation filter, BP: 480/40 nm, emission filter, BP 527/30 nm). After injection of 100 μl of FD, one stack of images was acquired before EP. Images were taken every 20 s for 2 min. The same procedure of image acquisition (every 20 s for 2 min) was performed immediately after EP. Immediately afterwards, a third stack of images was acquired in which images were taken every 2 min during 30 min. For experiments with 20 kDa FDs, due to its rapid clearance, the acquisition with 20 s time interval after EP was performed during 12 min. When injection of FD was performed after EP, two stacks were acquired consecutively just after the injection one stack of 2 min (at a 20 s repetition rate) and another one of 30 min (at a 2 min repetition rate). The files were stored and analyzed off-line with image acquisition and analysis software (Metavue, Metamorph, Molecular devices, Sunnyvale, CA, USA or AxioVision, Zeiss).

2.6. Data analysis

Increase in fluorescence intensity inside and outside the blood vessels was determined as follows. The "flattened background" option of image analysis software (Metavue or AxioVision) allowed for the correction of the image of filled blood vessels (before extravasation) for a non-uniform background. After this correction, by applying a suitable threshold on the image, the image was binarized and a mask of the vessel network was obtained. The tissues outside the vessels were defined by an inversion of the binarized mask of the vessel network. From these masks, the area of blood vessels and tissues was determined. After combination of the masks with all the aligned images of the acquired stacks, we determined the variation in fluorescence intensity inside and outside the vessels at all-time points after EP. The percentage of variations was calculated to avoid the variability between mice in the initial value of tissue fluorescence intensity. The time dependence of the obtained values during the first 3 min post EP was calculated to determine the initial mean fluorescence intensity changes per minute. When injection of FDs was performed after EP, the initial mean fluorescence intensity changes per minute were determined from the 3 min following a normal time of filling up of blood vessels (Fig. 1). The diameter of venules and arterioles was measured with AxioVision (Zeiss) software or Image J software (National Institute of Mental Health, Bethesda, MD, USA). Vessels were categorized as arterioles if they were narrow, straight and with few branches, and the others were defined as venules [33]. To measure diameters, at least five venules (diameters between 20 and 250 μm) and arterioles (10–100 μm) were selected from each mouse. Diameters of vessels were determined before application of electric pulses and thereafter every 20 s for the first 2 min and every 2 min for the rest of the acquisition time (30 min).

2.7. Statistical analysis

Statistical analysis was carried out using Prism 5 Statistical software (GraphPad Software Inc., San Diego, CA). For comparison of control and EP groups, Student t-tests were used, and for multiple comparisons, a one-way ANOVA with Dunnett's post-test. A value of $p < 0.05$ was considered to represent a significant difference between groups.

3. Results

3.1. Characterization of the DWC model: perfusion and clearance of FITC-labeled dextrans (FDs) in the blood vessels

In order to characterize if the perfusion of the blood vessels was independent of the molecular weight of the dextran, we first determined the kinetics of blood vessel filling after intravenous (i.v.) injections of FDs. Whatever the size of the dextran (20, 70 or 2000 kDa), the perfusion was completed within 120 s after the injection (Fig. 1A, Supplementary movie S1). Therefore, in all further experiments, EP was applied at 2 min after the injection of FDs.

We also determined the clearance of FDs from the blood stream and their long-term presence in the surrounding tissue. The clearance kinetics of FDs in intact vessels was dependent on their size. The larger FDs stayed in the blood stream for longer. The half time of clearance for 20 kDa FD was 8.5 min and for 70 and 2000 kDa FDs were greater than 4 h (5 h 30 min and 4 h, respectively) (Fig. 1B).

In order to study non-specific effects that could be induced by DWC surgery on vessel permeability, we measured the extravasation of 70 kDa FD from the blood vessels of a control mouse without EP, at different times after DWC implantation (Fig. 1C). The percentage of variation of mean fluorescence intensity in the tissues outside the vessels was very low and only slightly modified as a function of time during 15 days, indicating that implantation of DWC alone did not affect the permeability of vessels with time.
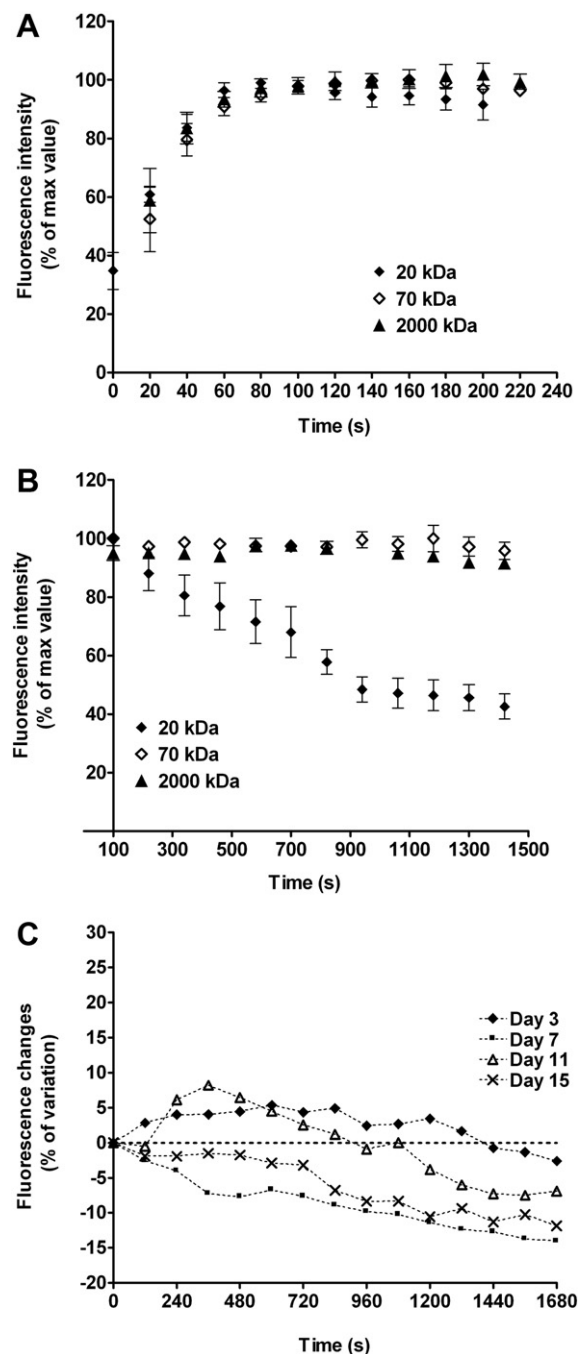

Fig. 1. Characterization of the DWC model. A — filling up of the blood vessels. Time course of mean fluorescence intensity changes in DWC vessels after 20, 70 and 2000 kDa FD injection B — elimination of the dextran. Mean fluorescence values were expressed as a % of the intensity, when the perfusion of vessels was totally completed. C — mean fluorescence intensity changes in DWC tissues with time. Measure of relative mean fluorescence intensity changes in DWC tissues outside the blood vessels in the same control mouse at different times after DWC implantation.

3.2. The EP-induced blood vessel permeability varies for different sizes of dextrans

In order to study the effects of EP on blood vessel permeability for different sizes of circulating molecules, we compared the extravasation of 20, 70 and 2000 kDa FDs from the blood vessels that were exposed to EP relative to control mice (no EP). The extravasation of 70 kDa FD induced by EP is illustrated in Fig. 2 (Supplementary movie S2), demonstrating a rapid leakage from all exposed blood vessels.
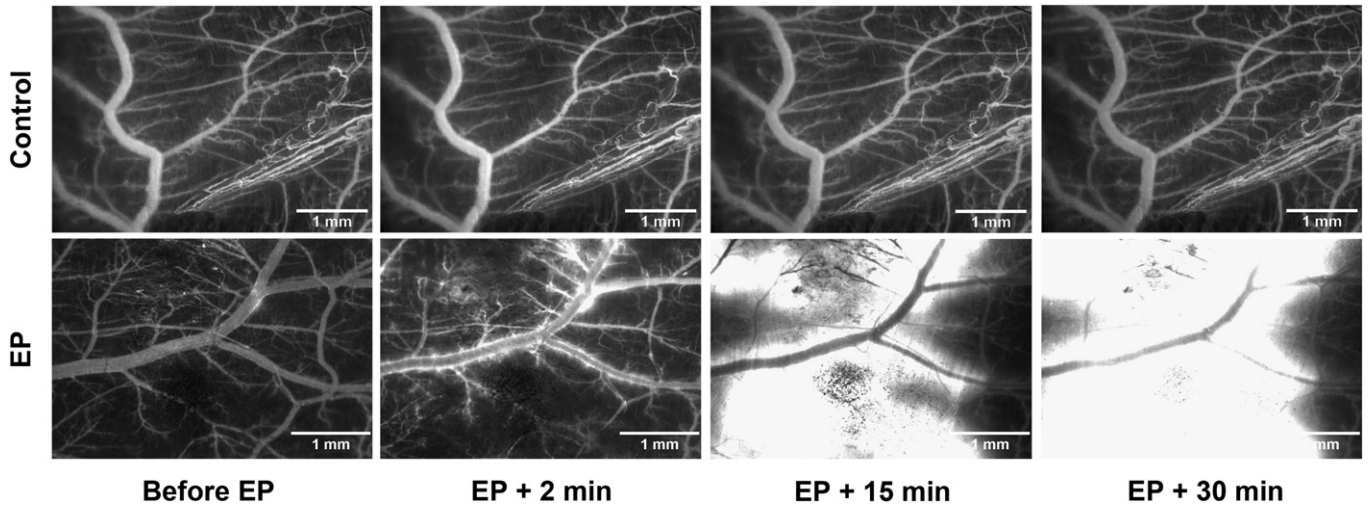
Fig. 2. Direct imaging of fluorescence leakage from the DWC vessels into tissues after EP. 70 kDa FD was injected i.v. and blood vessels were visualized by fluorescence macroscopy at ×25 magnification at the indicated times. Upper panel, no EP applied. Lower panel, eight square wave electric pulses, amplitude per distance 1300 V/cm, pulse length 100 µs at repetition frequency 1 Hz were applied.

The time course of extravasation was measured by the relative variation of mean fluorescence intensity in the tissue after EP (Fig. 3A). The relative variati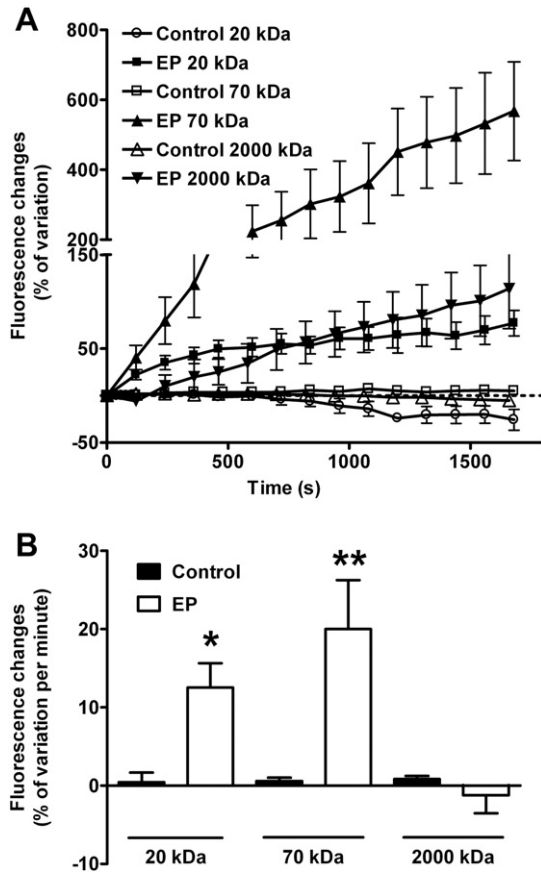on of mean fluorescence intensity was corrected by the vascular area (area of blood vessels) in the observed tissues of mice exposed to EP (see Materials and methods). For the 70 kDa FD, the increase was linearly dependent on time, as expected from the increase of vessel permeability present during the first minutes. For 2000 kDa FD, the same linear dependency was observed after the 3 min delay. However, the relative variation in mean fluorescence intensity was lower in comparison with 70 kDa FD (Fig. 3A). For 20 kDa FD, the increase in relative variation of mean fluorescence intensity reached a plateau value after 3 min (Fig. 3A).

For dextrans up to 70 kDa, a high and statistically significant increase in relative variation of mean fluorescence intensity per minute was obtained immediately after EP in comparison to control mice (Fig. 3B). For the 20 kDa FD, the fast clearance of dextran from the blood stream decreased the quantity of dextran available for leakage into the tissue, leading to a lower relative variation of mean fluorescence intensity per minute. In contrast, EP did not induce immediate leakage for 2000 kDa FD. Indeed, no modification of the relative variation of mean fluorescence intensity per minute was detected immediately after EP (Fig. 3B). However, after a delay (4 min), a significant increase in the variation of mean fluorescence intensity per minute, similar to the ones determined for smaller sizes of FDs, was quantified (10.9% +/− 4.7 of variation per min).

3.3. EP-induced blood vessel permeability is reversible

In order to determine the duration of the EP-induced permeability of blood vessels, we compared the extravasation of different FDs when injected at different times after EP (Fig. 4). The relative variation of mean fluorescence intensity per minute in the tissue quickly decreased when there was an increase in the delay interval between EP and 70 kDa FD injection. This suggested a quick partial restoration of blood vessel impermeability. However, the relative variation of mean fluorescence intensity per minute returned to the control level only 1 h post-EP (Fig. 4A). Similar data were observed with 2000 kDa FD (Fig. 4B).

We hypothesized that this delayed return to control level could be explained by a residual permeability to smaller molecules. Thus, we used intermediary times of injection (30 s, 5, 10, 20 and 30 min) with 20 kDa FD, to measure more precisely the lifetime of blood vessel increased permeability. In these conditions, the relative variation of mean fluorescence intensity per minute in the tissue remained constant at shorter time intervals (30 s, 5 min and 10 min) between EP and injection of FD (Fig. 4C).
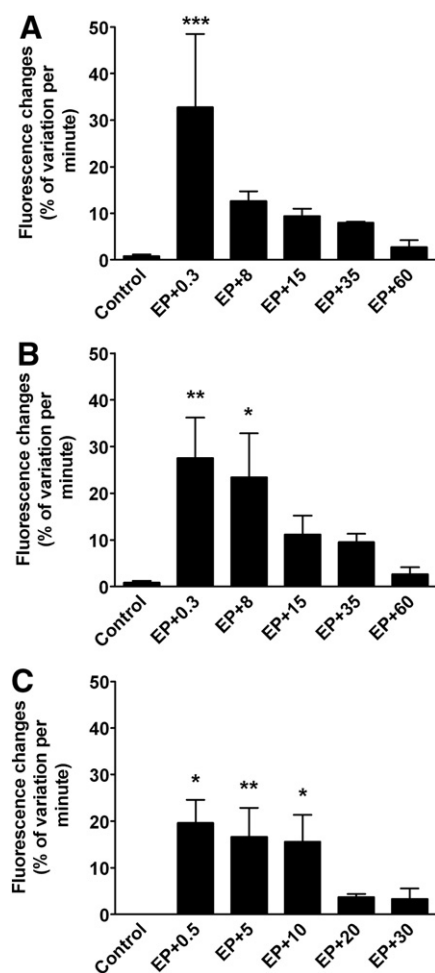

Fig. 3. Quantification of FD leakage kinetics after EP. (A): relative mean fluorescence intensity changes for 20, 70 and 2000 kDa FDs in DWC tissues outside the vessels as a function of time after EP (eight square wave electric pulses, amplitude per distance 1300 V/cm, pulse length 100 µs, repetition frequency 1 Hz, (n=6)), in comparison with the control group without EP (n=5). (B): initial relative mean fluorescence intensity changes per minute, determined from the first 3 min following EP for 20, 70 and 2000 kDa FDs (EP group (n=5), control group (n=4)). *P<0.05, **P<0.01 relative to pertinent control. Error bars indicate SEM.

Fig. 4. Duration of the EP-induced blood vessel permeability. Relative mean fluorescence intensity changes per minute in DWC tissues outside the vessels. Eight square electric pulses, amplitude 1300 V/cm, pulse length 100 μs, repetition frequency 1 Hz were applied and FD injection was performed at the indicated times. No EP was performed in controls. (A) 70 and (B) 2000 kDa FD injected 20 s, 8, 15, 35 and 60 min after EP, and (C) 20 kDa FD injected 30 s, 5 10, 20 and 30 min after EP. Three to five mice were tested for each experimental group. *P<0.05, **P<0.01, ***P<0.001 relative to control. Error bars indicate SEM.

This result suggested that the quick restoration of blood vessel impermeability observed with 70 and 2000 kDa FDs was indeed partial and did not prevent the leakage of smaller molecules during the first 10 min after EP.

3.4. EP induces vascular lock in normal blood vessels

Without EP, the filling up of blood vessels was immediate (within 2 min) with no leakage from blood vessels whatever the size of FD used (Fig. 1). When FDs were injected 20 s after EP, the filling up of pulsed blood vessels was slowed down whatever the size of the dextran (Fig. 5, Supplementary movie S3).

3.5. Duration of EP-induced vascular lock

In order to determine the duration of the vascular lock, FDs (20 and 2000 kDa) were injected at different times after EP. The percentage of mean fluorescence intensity inside blood vessels was plotted as a function of time (Fig. 6A and D). The shape of the curves clearly depended on the delay between EP and FD injection. To quantify this duration, we calculated their time derivatives. When the amplitude of the derivative was maximal, the vessel filling up speed was maximal. The maximal value of the derivative was determined for each condition

as the maximal variation of intensity per second (Fig. 6C and F). The delay between the time of injection (time 0) and time of the maximal derivative reflected the occurrence of blood vessels filling up. This delay was determined for each condition (Fig. 6B and E). For 20 kDa FD, the time needed to restore blood flow was at least 5 min (Fig. 6B). Ten minutes is needed to reach the normal rate of the blood flow (Fig 6C). In others words, these data showed that 5 min after EP, even if the blood flow was restored, its rate did not return to normal values until 10 min after EP. For 2000 kDa FD, the restoration of the blood flow was observed at least 15 min after EP. (Fig. 6E). The rates of blood flow were slightly decreased in comparison to normal value but not significantly (Fig 6F).

Therefore, the EP-induced vascular lock was detected over less than 10 min for 20 kDa FD and less than 15 min for 2000 kDa FD after EP.

3.6. Blood vessel constriction during EP-induced vascular lock

In order to characterize the EP-induced vascular lock, we measured the variation in the diameters of venules and arterioles during the first 30 min after EP. With 70 kDa FD, the increased permeability of blood vessels was associated with a constriction of both arterioles and venules. A small, but significant, constriction of venules (approx. 20%) was observed immediately after EP (Fig. 7B). The diameter of venules was totally restored 3 min after EP. Constriction of arterioles was more pronounced (approx. 65%) and mainly restored within 3 min after EP. However, the total restoration of their diameter was obtained after 8 min post-EP (Fig. 7A). The diameter of venules and arterioles in control mice were not modified during the same observation time. These results were not dependent on the FD's size (data not shown, Supplementary movie S4).

4. Discussion

This study presents the results of *in vivo* direct observations of the early events in blood vessels after EP in a DWC model in mice. Delivery of validated EP parameters used in clinical applications [29,30] to normal tissue (skin) led to a rapid increase in the permeability of blood vessels for different sizes of molecules that gradually returned to basal (control) levels within 1 h post-treatment. Moreover, EP induced an immediate constriction of blood vessels that was transient and returned to control levels within 8 min.

First, we characterized the DWC model. We showed that the filling up of the blood vessels (perfusion) was completed within 2 min after injection of FDs, in the absence of EP, whatever the size of the FD. FD injection did not modify the blood flow. A longer plasma elimination half-life and total blood clearance were detected for larger FDs (Fig. 1). This has already been observed in studies on children. Indeed, 2–3 h after injection, the main part of the dextran molecules still circulating in the blood flow had a molecular weight of 30–50 kDa or more. Smaller molecules had already by this time been excreted into the urine [34].

Our experimental setting using the DWC model in mice, allowed direct observation of blood vessels *in vivo*. As such, we could measure *in situ* the changes in blood vessel permeability after EP, in real time. Molecules (up to 70 kDa) were used as model molecules for drugs and oligonucleotides whilst 2000 kDa FD has a molecular size comparable to plasmid DNA [35,36]. We showed an occurrence of vascular permeability immediately after EP for 20 and 70 kDa FDs (Figs. 2 and 3). For 2000 kDa FD, this occurrence of permeability was delayed in time (4 min). Therefore, permeability was observed for all three sizes of FDs (20 kDa, 70 kDa and 2000 kDa) that in normal circumstances do not diffuse readily through vessel walls [37]. Vascular impermeability was partially restored within 10 min for all sizes of FDs, whilst a low level of leakage was still present after this time. The impermeability of vessels totally returned to basal values within 1 h after EP (Fig. 4).
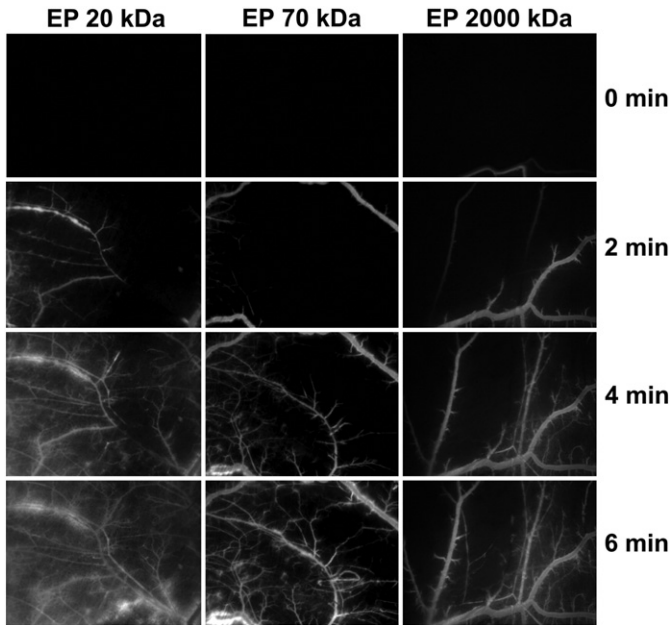
Fig. 5. Illustration of the EP-induced vascular lock. Eight square wave electric pulses, amplitude 1300 V/cm, pulse length 100 µs, repetition frequency 1 Hz were applied. 20, 70 and 2000 kDa FDs were injected 20 s after EP. DWC were observed by fluorescence macroscopy and images were acquired immediately after (0 min), 2, 4 and 6 min after FDs injection.

A direct consequence of these findings is that, once injected intravenously, plasmid DNA could mostly be delivered to the tissue between 3 and 10 min after EP. Now, plasmid DNA must be present during the application of electric pulses in order to be efficiently transferred into the cells because of the involvement of electrophoretic forces [12,35,38]. Therefore, skin transfection after intravenous plasmid DNA injection could be impeded because of this delayed vascular permeability that we observed with 2000 kDa FD. This delay explains the very low level of transfection in the skin after intravenous plasmid DNA injection reported elsewhere [28].

The permeability of blood vessels for 70 kDa FD was slightly higher than for 2000 kDa FD whereas, for the 20 kDa FD, the results were slightly lower (Fig. 3). This was due to its quick clearance out of the blood stream (8.5 min) (Fig. 1B). Molecules in size up to 70 kDa could diffuse easier into the tissue after EP than much larger ones such as 2000 kDa FD. The increased vascular permeability is due to the structural changes in the blood vessels' wall that are caused by a direct effect of EP on the endothelial lineage present in arterioles and venules [27]. Previously published results on endothelial cells *in vitro* showed reversible structural changes of the cytoskeleton and cell junctions concomitant with a rapid rise in endothelial monolayer permeability [26]. Nevertheless, the full restoration of blood vessel permeability, observed in our study, confirmed that no endothelial cells were irreversibly damaged by the validated EP parameters *in vivo*. The effects of irreversible electroporation (IRE) on blood vessels by applying stronger EP parameters than in our study (10 pulses of 100 µs, 3800 V/cm, 10 Hz) showed that in large vessels only the vascular smooth muscle cells were affected at day 28 post-treatment [39]. However in our study we provide evidence that the application of validated EP parameters used in clinical applications [29,30] does not harm small vessels (arterioles, venules and capillaries). Therefore, we provide additional proof of the safety of EP, when applied to normal tissues. Although mouse skin has different physiological and anatomical properties compared to human skin, several studies have demonstrated that the effects of EP observed in mouse studies were also confirmed in preclinical studies in higher mammals (pigs) and in clinical studies in humans [40–42].

The immediate and transient constriction of blood vessels that we observed was in agreement with global observations of reduced perfusion measured by Gehl et al. using Patent Blue staining *in vivo* in normal muscle tissue after EP [19]. A first phase of vascular response to EP was attributed to sympathetically-mediated vasoconstriction acting on smooth muscles of afferent arterioles, leading to a rapid and profound but short-lived initial decrease in blood flow. Arterioles have a thick vessel wall with a *Tunica Media* composed of several layers of circular smooth muscles, whereas veins and venules have a thinner layer of circular smooth muscles. Following the hypothesis of sympathetically-mediated vasoconstriction, these different morphologies should make arterioles more sensitive to EP than venules. Our measurements of blood vessel diameters provide direct evidence of the different levels of vasoconstriction of venules and arterioles Namely, the constriction of venules was minor (~20%), a level significant only immediately after EP (1 min), and was restored to its basal level within 3 min. The constriction of arterioles was more profound (~65%) and long lasting (8 min) (Fig. 7). These vasoconstrictions resulted in the "vascular lock" (Fig. 5). In the proposed model of vasoconstriction in mouse muscle, a second phase was attributed to the permeabilization of muscle fibers and endothelial cell membranes leading to increased interstitial pressure and decreased intravascular pressure, which could explain delay of perfusion in muscles [19]. Additionally, we determined that the filling up of pulsed blood vessels was slightly different for various sizes of FDs (Fig. 6). Furthermore, our results also demonstrate that the delivery of large molecules (2000 kDa) to the tissues was delayed (Figs. 3A, 5). Indeed, when 2000 kDa FD was already present
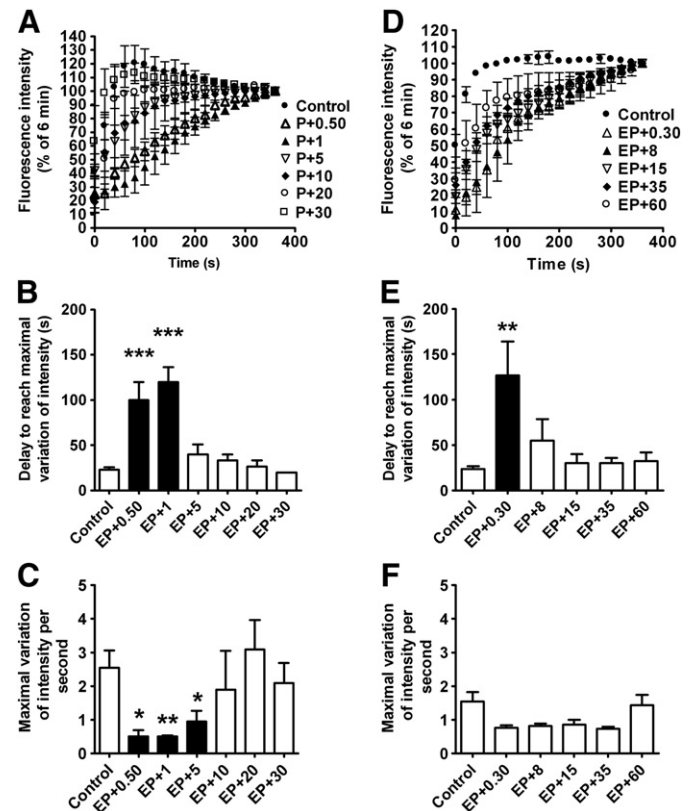

Fig. 6. Quantification of vascular lock after EP. Eight square wave electric pulses, amplitude per distance 1300 V/cm, pulse length 100 µs, repetition frequency 1 Hz, were applied. 20 or 2000 kDa FITC-dextran was injected at different times after EP, and compared to the control. (A, D) The fluorescence intensity as a percentage relative to the 6 min value is plotted as a function of time for 20 and 2000 kDa dextran, respectively. Derivatives of (A, D) curves, respectively, were calculated. (B, E) Delay of the occurrence of the maximal derivative was determined for each condition (B — 20 kDa, E — 2000 kDa FD). (C, F) Amplitude of the maximal derivative value was plotted for each condition (C — 20 kDa, F — 2000 kDa FD). *P<0.05, **P<0.01, ***P<0.001 relative to control. Error bars indicate SEM.
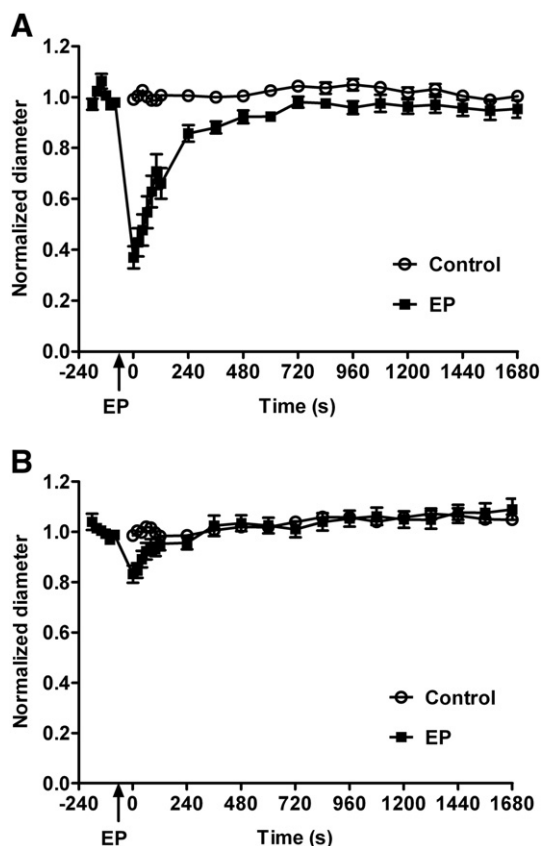
Fig. 7. Time course of blood vessel diameter changes. Blood vessels were visualized by 70 kDa FD injection and their diameters were normalized to the initial value before EP. Normalized diameters of arterioles (A) and venules (B) were plotted as a function of time after EP (eight square wave electric pulses, amplitude per distance 1300 V/cm, pulse length 100 μs, repetition frequency 1 Hz, (n = 5)) in comparison with the control group without EP (n = 5). Error bars indicate SEM.

in the blood stream, the extravasation induced by EP was delayed compared to smaller FDs and began ~4 min after EP.

To the best of our knowledge, this study is the first report of direct observation of EP-induced increased permeability of vessels *in vivo* with validated electric pulses used for biomedical applications according to the size of dextrans. We were able to gain an insight into the physiological processes that were altered by EP of the tissues, that had before only been the subject of speculation [19,24,43].

5. Conclusions

The increased leakage of different sizes of FDs indicated that EP-induced permeability of the vasculature could be effective for a broad range of molecules such as oligonucleotides and plasmid DNA. For small molecules (20 kDa FD) because of their rapid elimination EP has to be performed rapidly after the injection. If performed after EP, the injection has to be undertaken within 10 min. In support to this, in ECT with cisplatin, the antitumor effect was still pronounced when cisplatin was injected 10 min after EP [44]. For dextrans above 70 kDa, their slow clearance and the linear increase in extravasation after EP suggest that, after injection of large molecules, EP can be applied after a longer time interval, resulting in the same amount of delivered molecules into the target tissue. Finally, the delayed permeability observed with 2000 kDa FD suggests that very large molecules such as plasmid DNA are more sensitive to vascular lock. Indeed, arteriole constriction delays 2000 kDa molecule extravasation, whereas leakage of smaller molecules is not impeded. Thus, knowledge of the vascular effects of EP can lead to a better planning of the treatments

that are based on EP (electrochemotherapy, electrogene therapy and DNA vaccination) for increased efficacy of treatment or for distribution of the i.v. injected molecules (*i.e.* drugs, siRNA, plasmid DNA) [28,45–48].

Supplementary data to this article can be found online at http://dx.doi.org/10.1016/j.jconrel.2012.09.010.

References

[1] L.M. Mir, S. Orlowski, Mechanisms of electrochemotherapy, Adv. Drug Deliv. Rev. 35 (1999) 107–118.
[2] M. Cemazar, M. Golzio, G. Sersa, M.P. Rols, J. Teissie, Electrically-assisted nucleic acids delivery to tissues *in vivo*: where do we stand? Curr. Pharm. Des. 12 (2006) 3817–3825.
[3] R. Heller, M.J. Jaroszeski, L.F. Glass, J.L. Messina, D.P. Rapaport, R.C. DeConti, N.A. Fenske, R.A. Gilbert, L.M. Mir, D.S. Reintgen, Phase I/II trial for the treatment of cutaneous and subcutaneous tumors using electrochemotherapy, Cancer 77 (1996) 964–971.
[4] L.M. Mir, C. Roth, S. Orlowski, F. Quintin-Colonna, D. Fradelizi, J. Belehradek Jr., P. Kourilsky, Systemic antitumor effects of electrochemotherapy combined with histoincompatible cells secreting interleukin-2, J. Immunother. Emphasis Tumor Immunol. 17 (1995) 30–38.
[5] G. Sersa, D. Miklavcic, M. Cemazar, Z. Rudolf, G. Pucihar, M. Snoj, Electrochemotherapy in treatment of tumours, Eur. J. Surg. Oncol. 34 (2008) 232–240.
[6] M. Belehradek, C. Domenge, B. Luboinski, S. Orlowski, J. Belehradek Jr., L.M. Mir, Electrochemotherapy, a new antitumor treatment. First clinical phase I–II trial, Cancer 72 (1993) 3694–3700.
[7] J. Gehl, P.F. Geertsen, Efficient palliation of haemorrhaging malignant melanoma skin metastases by electrochemotherapy, Melanoma Res. 10 (2000) 585–589.
[8] R. Heller, M.J. Jaroszeski, D.S. Reintgen, C.A. Puleo, R.C. DeConti, R.A. Gilbert, L.F. Glass, Treatment of cutaneous and subcutaneous tumors with electrochemotherapy using intralesional bleomycin, Cancer 83 (1998) 148–157.
[9] Y. Kubota, T. Nakada, H. Yanai, K. Itoh, I. Sasagawa, K. Kawai, Histological evaluation of the effects of electropermeabilization after administration of bleomycin on bladder cancer in the rat, Eur. Urol. 34 (1998) 372–376.
[10] G. Sersa, B. Stabuc, M. Cemazar, D. Miklavcic, Z. Rudolf, Electrochemotherapy with cisplatin: the systemic antitumour effectiveness of cisplatin can be potentiated locally by the application of electric pulses in the treatment of malignant melanoma skin metastases, Melanoma Res. 10 (2000) 381–385.
[11] M. Cemazar, T. Jarm, G. Sersa, Cancer electrogene therapy with interleukin-12, Curr. Gene. Ther. 10 (2010) 300–311.
[12] J.M. Escoffre, J. Teissie, M.P. Rols, Gene transfer: how can the biological barriers be overcome? J. Membr. Biol. 236 (2010) 61–74.
[13] M. Golzio, J.M. Escoffre, T. Portet, C. Mauroy, J. Teissie, D.S. Dean, M.P. Rols, Observations of the mechanisms of electromediated DNA uptake — from vesicles to tissues, Curr. Gene. Ther. 10 (2010) 256–266.
[14] T. Matsuda, C.L. Cepko, Controlled expression of transgenes introduced by *in vivo* electroporation, Proc. Natl. Acad. Sci. U. S. A. 104 (2007) 1027–1032.
[15] D. Pavlin, M. Cemazar, A. Cör, G. Sersa, A. Pogacnick, N. Tozon, Electrogene therapy with interleukin-12 in canine mast cell tumors, Radiol. Oncol. 45 (2011) 31–39.
[16] S. Vidic, B. Markelc, G. Sersa, A. Coer, U. Kamensek, G. Tevz, S. Kranjc, M. Cemazar, MicroRNAs targeting mutant K-ras by electrotransfer inhibit human colorectal adenocarcinoma cell growth *in vitro* and *in vivo*, Cancer Gene. Ther. 17 (2010) 409–419.
[17] A.I. Daud, R.C. DeConti, S. Andrews, P. Urbas, A.I. Riker, V.K. Sondak, P.N. Munster, D.M. Sullivan, K.E. Ugen, J.L. Messina, R. Heller, Phase I trial of interleukin-12 plasmid electroporation in patients with metastatic melanoma, J. Clin. Oncol. 26 (2008) 5896–5903.
[18] L.C. Heller, R. Heller, Electroporation gene therapy preclinical and clinical trials for melanoma, Curr. Gene. Ther. 10 (2010) 312–317.
[19] J. Gehl, T. Skovsgaard, L.M. Mir, Vascular reactions to in vivo electroporation: characterization and consequences for drug and gene delivery, Biochim. Biophys. Acta 1569 (2002) 51–58.

[20] L.H. Ramirez, S. Orlowski, D. An, G. Bindoula, R. Dzodic, P. Ardouin, C. Bognel, J. Belehradek Jr., J.N. Munck, L.M. Mir, Electrochemotherapy on liver tumours in rabbits, Br. J. Cancer 77 (1998) 2104–2111.

[21] G. Sersa, K. Beravs, M. Cemazar, D. Miklavcic, F. Demsar, Contrast enhanced MRI assessment of tumor blood volume after application of electric pulses, Electro- Magnetobiol. 17 (1998) 299–306.

[22] T. Ivanusa, K. Beravs, M. Cemazar, V. Jevtic, F. Demsar, G. Sersa, MRI macromolecular contrast agents as indicators of changed tumor blood flow, Radiol. Oncol. 35 (2001) 139–147.

[23] G. Sersa, M. Cemazar, D. Miklavcic, D.J. Chaplin, Tumor blood flow modifying effect of electrochemotherapy with bleomycin, Anticancer Res. 19 (1999) 4017–4022.

[24] G. Sersa, M. Cemazar, C.S. Parkins, D.J. Chaplin, Tumour blood flow changes induced by application of electric pulses, Eur. J. Cancer 35 (1999) 672–677.

[25] G. Sersa, T. Jarm, T. Kotnik, A. Coer, M. Podkrajsek, M. Sentjurc, D. Miklavcic, M. Kadivec, S. Kranjc, A. Secerov, M. Cemazar, Vascular disrupting action of electroporation and electrochemotherapy with bleomycin in murine sarcoma, Br. J. Cancer 98 (2008) 388–398.

[26] C. Kanthou, S. Kranjc, G. Sersa, G. Tozer, A. Zupanic, M. Cemazar, The endothelial cytoskeleton as a target of electroporation-based therapies, Mol. Cancer Ther. 5 (2006) 3145–3152.

[27] B. Markelc, E. Bellard, G. Sersa, S. Pelofy, J. Teissie, A. Coer, M. Golzio, M. Cemazar, In vivo molecular imaging and histological analysis of changes induced by electric pulses used for plasmid DNA electrotransfer to the skin: a study in a dorsal window chamber in mice, J. Membr. Biol. 245 (9) (2012) 545–554.

[28] O. Thanaketpaisarn, M. Nishikawa, F. Yamashita, M. Hashida, Tissue-specific characteristics of in vivo electric gene: transfer by tissue and intravenous injection of plasmid DNA, Pharm. Res. 22 (2005) 883–891.

[29] M. Marty, G. Sersa, J.R. Garbay, J. Gehl, C.G. Collins, M. Snoj, V. Billard, P.F. Geertsen, J.O. Larkin, D. Miklavcic, I. Pavlovic, S.M. Paulin-Kosir, M. Cemazar, N. Morsli, D.M. Soden, Z. Rudolf, C. Robert, G.C. O'Sullivan, L.M. Mir, Electrochemotherapy — an easy, highly effective and safe treatment of cutaneous and subcutaneous metastases: results of ESOPE (European Standard Operating Procedures of Electrochemotherapy) study, Eur. J. Cancer Suppl. (2006) 3–13.

[30] L.M. Mir, J. Gehl, G. Sersa, C.G. Collins, J.R. Garbay, V. Billard, P.F. Geertsen, Z. Rudolf, G.C. O'Sullivan, M. Marty, Standard operating procedures of the electrochemotherapy: Instructions for the use of bleomycin or cisplatin administered either systemically or locally and electric pulses delivered by the cliniporator™ by means of invasive or non-invasive electrodes, Eur. J. Cancer Suppl. (2006) 14–25.

[31] M.R. Dreher, W. Liu, C.R. Michelich, M.W. Dewhirst, F. Yuan, A. Chilkoti, Tumor vascular permeability, accumulation, and penetration of macromolecular drug carriers, J. Natl. Cancer Inst. 98 (2006) 335–344.

[32] G.M. Palmer, A.N. Fontanella, S. Shan, G. Hanna, G. Zhang, C.L. Fraser, M.W. Dewhirst, In vivo optical molecular imaging and analysis in mice using dorsal window chamber models applied to hypoxia, vasculature and fluorescent reporters, Nat. Protoc. 6 (2011) 1355–1366.

[33] G.M. Tozer, V.E. Prise, J. Wilson, M. Cemazar, S. Shan, M.W. Dewhirst, P.R. Barber, B. Vojnovic, D.J. Chaplin, Mechanisms associated with tumor vascular shut-down induced by combretastatin A-4 phosphate: intravital microscopy and measurement of vascular permeability, Cancer Res. 61 (2001) 6413–6422.

[34] G. Arturson, G. Wallenius, The renal clearance of dextran of different molecular sizes in normal humans, Scand. J. Clin. Lab. Invest. 16 (1964) 81–86.

[35] M. Golzio, J. Teissie, M.P. Rols, Direct visualization at the single-cell level of electrically mediated gene delivery, Proc. Natl. Acad. Sci. U. S. A. 99 (2002) 1292–1297.

[36] A. Paganin-Gioanni, E. Bellard, J.M. Escoffre, M.P. Rols, J. Teissie, M. Golzio, Direct visualization at the single-cell level of siRNA electrotransfer into cancer cells, Proc. Natl. Acad. Sci. U. S. A. 108 (2011) 10443–10447.

[37] Y. Takakura, M. Hashida, Macromolecular carrier systems for targeted drug delivery: pharmacokinetic considerations on biodistribution, Pharm. Res. 13 (1996) 820–831.

[38] M. Cemazar, D. Pavlin, S. Kranjc, A. Grosel, S. Mesojednik, G. Sersa, Sequence and time dependence of transfection efficiency of electrically-assisted gene delivery to tumors in mice, Curr. Drug Deliv. 3 (2006) 77–81.

[39] E. Maor, A. Ivorra, J. Leor, B. Rubinsky, The effect of irreversible electroporation on blood vessels, Technol. Cancer Res. Treat. 6 (2007) 307–312.

[40] A.R. Denet, R. Vanbever, V. Preat, Skin electroporation for transdermal and topical delivery, Adv. Drug Deliv. Rev. 56 (2004) 659–674.

[41] A. Gothelf, F. Mahmood, F. Dagnaes-Hansen, J. Gehl, Efficacy of transgene expression in porcine skin as a function of electrode choice, Bioelectrochemistry 82 (2011) 95–102.

[42] G. Sersa, T. Cufer, S.M. Paulin, M. Cemazar, M. Snoj, Electrochemotherapy of chest wall breast cancer recurrence, Cancer Treat. Rev. 38 (2012) 379–386.

[43] T. Jarm, M. Cemazar, D. Miklavcic, G. Sersa, Antivascular effects of electrochemotherapy: implications in treatment of bleeding metastases, Expert. Rev. Anticancer. Ther. 10 (2010) 729–746.

[44] G. Sersa, M. Cemazar, D. Miklavcic, Antitumor effectiveness of electrochemotherapy with cis-diamminedichloroplatinum(II) in mice, Cancer Res. 55 (1995) 3450–3455.

[45] I. Edhemovic, E.M. Gadzijev, E. Brecelj, D. Miklavcic, B. Kos, A. Zupanic, B. Mali, T. Jarm, D. Pavliha, M. Marcan, G. Gasljevic, V. Gorjup, M. Music, T.P. Vavpotic, M. Cemazar, M. Snoj, G. Sersa, Electrochemotherapy: a new technological approach in treatment of metastases in the liver, Technol. Cancer Res. Treat. 10 (2011) 475–485.

[46] B. Ferraro, M.P. Morrow, N.A. Hutnick, T.H. Shin, C.E. Lucke, D.B. Weiner, Clinical applications of DNA vaccines: current progress, Clin. Infect. Dis. 53 (2011) 296–302.

[47] D. Miklavcic, M. Snoj, A. Zupanic, B. Kos, M. Cemazar, M. Kropivnik, M. Bracko, T. Pecnik, E. Gadzijev, G. Sersa, Towards treatment planning and treatment of deep-seated solid tumors by electrochemotherapy, Biomed. Eng. Online 9 (2010) 10.

[48] M. Rosati, C. Bergamaschi, A. Valentin, V. Kulkarni, R. Jalah, C. Alicea, V. Patel, A.S. von Gegerfelt, D.C. Montefiori, D.J. Venzon, A.S. Khan, R. Draghia-Akli, K.K. Van Rompay, B.K. Felber, G.N. Pavlakis, DNA vaccination in rhesus macaques induces potent immune responses and decreases acute and chronic viremia after SIVmac251 challenge, Proc. Natl. Acad. Sci. U. S. A. 106 (2009) 15831–15836.